# PRELIMINARY COMPARISON BETWEEN OPENFOAM AND NON-HYDROSTATIC MODEL FOR WAVE-STRUCTURE INTERACTION

YUXIANG MA[1], CONGFANG AI[1], GUOHAI DONG[1]

[1]*State Key Laboratory of Coastal and Offshore Engineering, Dalian University of Technology,*
*yuxma@126.com*
*aicongfang@dlue.edu.cn*
*ghdong_dut@yeah.net*

**Abstract**
This study conducts comparison between the OpenFOAM and a non-hydrostatic free surface model for predicting wave-structure interactions. The non-hydrostatic model solves the incompressible Navier-Stokes equations based on a grid system, which is built from a horizontal rectangular grid by adding dozens of horizontal layers. The immersed boundary method is incorporated in the model to deal with structures. The results from the comparisons are provided for solitary wave interacting with a floating rectangular obstacle.

*Keywords: Wave-structure interaction; Immersed boundary method; OpenFOAM; Non-hydrostatic model*

## Introduction

Wave-structure interaction has been an important issue for a very long time. For structural design and safety assessment, it is of considerable interest for researchers to present accurate predictions of wave transmission and reflection induced by structure or wave forces exerted on the structure. Offshore structures exposed to open water in coastal areas may be various types including floating, suspended and bottom-mounted structures. It would be best to develop numerical models that are capable of predicting interaction between wave and any type of structure.

The so-called non-hydrostatic models are based on Navier-Stokes equations (NSE), but they treat the free surface elevation as a single-valued function of horizontal position. With the use of a free-surface equation to track the moving water surface, non-hydrostatic models are relatively computationally efficient. They have been widely used in the predictions of short surface waves (Ai, et al., 2014; Ai and Jin, 2012; Ai, et al., 2011; Ma et al., 2012; Zijlema et al., 2011), internal waves (Ai and Ding, 2016; Lai et al., 2010; Matsumura and Hasumi, 2008; Vitousek and Fringer, 2014) and even wave-structure interactions (Ai and Jin, 2010; Ai, et al., 2016; Lin, 2006; Ma et al. 2016).

In contrast to the OpenFOAM, non-hydrostatic model is computationally efficient because it does not need to capture the moving free surface with a large number of vertical grids. However, non-hydrostatic model cannot deal with overturning flow.

## Numerical models

InterFoam solver in OpenFOAM solving the NSE equations for both of the phases, water and air was used here. Details about the InterFoam solver can be referred to relating references and were not provided for brevity.

The 3D non-hydrostatic free surface flow is governed by the incompressible NSE, which can be written in the following form, by splitting the pressure into hydrostatic and non-hydrostatic ones, $p = \rho g(\eta - z) + \rho q$

$$\frac{\partial u}{\partial x} + \frac{\partial v}{\partial y} + \frac{\partial w}{\partial z} = 0 \tag{1}$$

$$\frac{\partial u}{\partial t} + \frac{\partial u^2}{\partial x} + \frac{\partial uv}{\partial y} + \frac{\partial uw}{\partial z} = -g\frac{\partial \eta}{\partial x} - \frac{1}{\rho}\frac{\partial q}{\partial x} + \frac{\partial}{\partial x}\left(\nu_t \frac{\partial u}{\partial x}\right) + \frac{\partial}{\partial y}\left(\nu_t \frac{\partial u}{\partial y}\right) + \frac{\partial}{\partial z}\left(\nu_t \frac{\partial u}{\partial z}\right) \tag{2}$$

$$\frac{\partial v}{\partial t} + \frac{\partial uv}{\partial x} + \frac{\partial v^2}{\partial y} + \frac{\partial vw}{\partial z} = -g\frac{\partial \eta}{\partial y} - \frac{1}{\rho}\frac{\partial q}{\partial y} + \frac{\partial}{\partial x}\left(\nu_t \frac{\partial v}{\partial x}\right) + \frac{\partial}{\partial y}\left(\nu_t \frac{\partial v}{\partial y}\right) + \frac{\partial}{\partial z}\left(\nu_t \frac{\partial v}{\partial z}\right) \tag{3}$$

$$\frac{\partial w}{\partial t} + \frac{\partial uw}{\partial x} + \frac{\partial vw}{\partial y} + \frac{\partial w^2}{\partial z} = -\frac{1}{\rho}\frac{\partial q}{\partial z} + \frac{\partial}{\partial x}\left(\nu_t \frac{\partial w}{\partial x}\right) + \frac{\partial}{\partial y}\left(\nu_t \frac{\partial w}{\partial y}\right) + \frac{\partial}{\partial z}\left(\nu_t \frac{\partial w}{\partial z}\right) \tag{4}$$

where $t$ is the time; $u$, $v$ and $w$ are the velocities in the $x$, $y$, and $z$ direction, respectively; $p$ is the pressure; $\eta$ is the free surface elevation; $q$ is the non-hydrostatic pressure component; $g$ is the gravitational acceleration; and $\nu_t$ is the eddy kinematic viscosity.

Here, the turbulent eddy viscosity $\nu_t$ is evaluated by using the Smagorinsky's subgrid scale model (Smagorinsky, 1963). To calculate the moving free surface, the following free surface equation is employed.

$$\frac{\partial \eta}{\partial t} + \frac{\partial}{\partial x}\int_{z=-h(x,y)}^{z=\eta(x,y,t)} u\, dz + \frac{\partial}{\partial y}\int_{z=-h(x,y)}^{z=\eta(x,y,t)} v\, dz = 0 \tag{5}$$

where $z = -h(x, y)$ is the bottom surface and $z = -\eta(x, y, t)$ is the free surface.

For the non-hydrostatic model, the overall numerical algorithm consists of the following two steps.

The first step is to solve the NSE by using an explicit projection method, which is subdivided into two stages (Ai, Jin and Lv, 2011). The first stage is to project intermediate velocities by means of solving the momentum equations that contain the non-hydrostatic pressure at the previous time level. In this stage, to get a momentum conservative scheme in the discretization of the advection terms, the Eqs. 1~4 are firstly integrated over a vertical layer. Then, the resulting

momentum equations in question are obtained by subtracting the integrated continuity equation from the integrated momentum equations. Finally, a finite volume method with a combination of first-order upwind scheme and second-order central differencing scheme is used to discretize the advection terms of the momentum equations. In the second stage, the new velocities are computed by correcting the projected values after including the non-hydrostatic pressure terms, which are obtained by solving the discretized Poisson equation. The Poisson equation is symmetric and positive definite and can be solved efficiently using the preconditioned conjugate gradient method.

In the second step, by substituting the resulting velocities into a discretized form of the free surface equation (5), we can obtain the new free surface elevation.

In the non-hydrostatic model, the immersed boundary method is used to deal with submerged structure. In this method, the structure is treated as virtual body and replaced by immersed boundary forces imposed on its boundary. Details about the immersed boundary method can be referred to Fadlun et al. (2000).

### Numerical reslts: Solitary wave interacting with a floating rectangular obstacle

The first test designed by Lin (2006) concerns interactions between solitary wave and a floating structure. In the test, the still water depth is $h = 1.0$ m and the incoming solitary wave has a wave height $H_0 = 0.1$ m. The computational domain in the $x$ direction ranges from 0 m to 100 m. A rectangular obstacle with dimensions of 5.0 m×0.6 m floats on the top of the water. The center of the obstacle is located at (32.5 m, 0.9 m). A schematic diagram showing solitary wave past a floating rectangular obstacle is depicted in Fig. 1.

In the computation, the computational domain is discretized by 1000 horizontal grids and 40 layers in the vertical direction. The time step is set to $\Delta t = 0.005$. Comparisons of time histories of the free surface elevation at $x = 1$ m and 59 m among present results and other model results are plotted in Fig. 2. In the simulations, all of the models ignored viscous effect. At the first gauging point ($x = 1$ m), the incident solitary wave and reflected waves are recorded. At the other gauging point ($x = 59$ m), the transmitted wave with reduced height is observed. The non-hydrostatic model results are in good agreement with both other model results. Fig. 3 shows comparisons of time histories of the horizontal and vertical forces exerted on the obstacle between present model results and OpenFOAM results. Good agreements can be observed for both the horizontal and vertical forces, although the present model slightly overpredicts the horizontal maximum positive and maximum negative forces. Fig. 4 shows non-hydrostatic model results of the vortex development during the process of solitary wave past the obstacle. It can be seen that a small vortex first forms near the bottom left of the obstacle, and then the other vortex is generated behind it. Both vortices persist for a very long time.
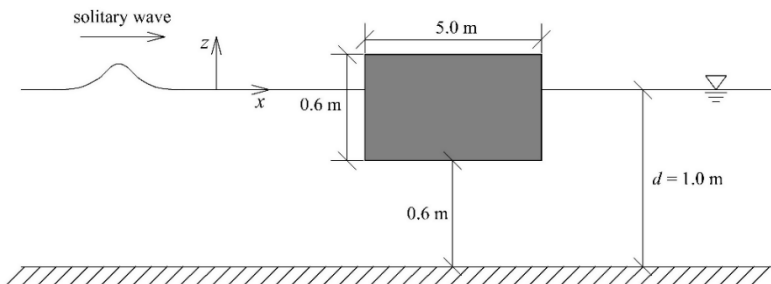


**Figure 1: Schematic diagram showing solitary wave past a floating rectangular obstacle**
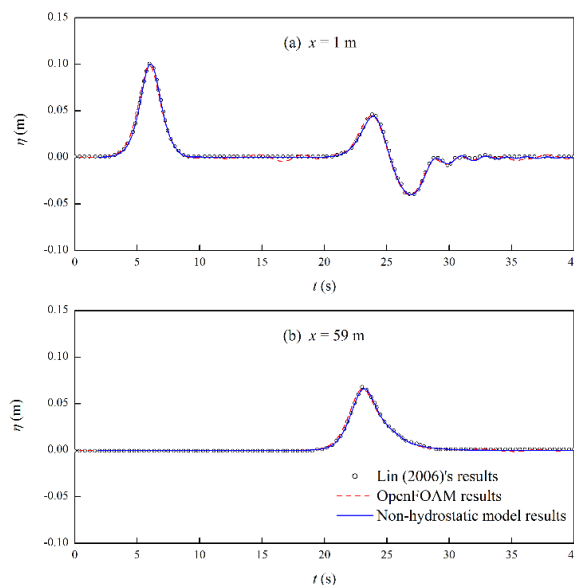


**Figure 2: Comparisons of time histories of free surface elevation among non-hydrostatic model results, results published by Lin (2006) and OpenFOAM results**

351
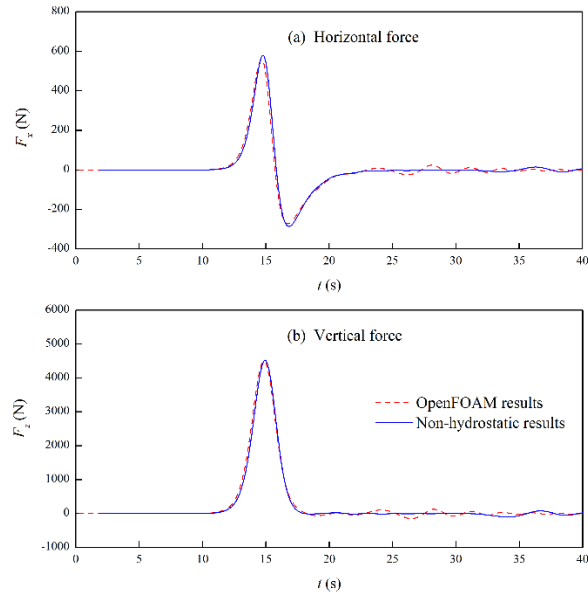
**Figure 3: Comparisons of time histories of the horizontal and vertical forces exerted on the obstacle between non-hydrostatic model results and OpenFOAM results**
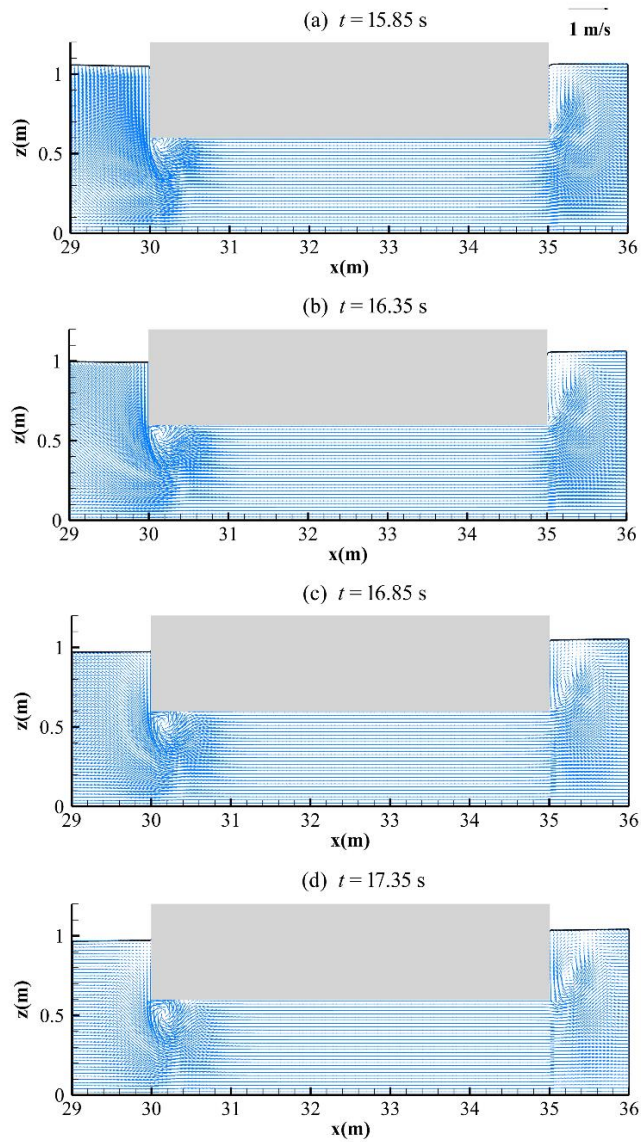


**Figure 4: Velocity fields around the obstacle during solitary wave past a floating rectangular obstacle**

## Conclusions

This paper presents preliminary comparison between OpenFOAM and non-hydrostatic model for wave-structure interaction. It is shown that the two models show very similar results of of free surface elevation and wave force exerted on structure. It can concluded that the non-hydrostatic model is comparable to the OpenFOAM in the wave-structure interactions involving single-valued free-surface flows.

## Acknowledgements

## References

[1]  Ai, C., Ding, W., 2016. A 3D unstructured non-hydrostatic ocean model for internal waves. Ocean Dyn. 66, 1253-1270.

[2]  Ai, C., Ding, W., Jin, S., 2014. A general boundary-fitted 3D non-hydrostatic model for nonlinear focusing wave groups. Ocean Eng. 89, 134-145.

[3]  Ai, C., Jin, S., 2010. Non-hydrostatic finite volume model for non-linear waves interacting with structures. Comput. Fluids 39, 2090-2100.

[4]  Ai, C., Jin, S., 2012. A multi-layer non-hydrostatic model for wave breaking and run-up. Coast. Eng. 62, 1-8.

[5]  Ai, C., Ding, W., Jin, S., 2017. A hybrid-grid 3D model for regular waves interacting with cylinders. J. Hydraul. Res. 55, 129-134.

[6]  Ai, C., Jin, S., Lv, B., 2011. A new fully non-hydrostatic 3D free surface flow model for water wave motions. Int. J. Numer. Method Fluids 66, 1354-1370.

[7]  Fadlun, E.A., Verzicco, R., Orlandi, P., Mohd-Yusof, J., 2000. Combined immersed boundary finite-difference methods for three-dimensional complex flow simulations. J. Comput. Phys. 161, 35-60.

[8]  Lai, Z., Chen, C., Cowles, G.W., Beardsley, R.C., 2010. A nonhydrostatic version of FVCOM: 1. Validation experiments. J. Geophys. Res. 115, C11010.

[9]  Lin, P., 2006. A multiple-layer coordinate model for simulation of wave-structure interaction. Comput. Fluids 35, 147-167.

[10] Ma, G., Farahani, A.A., Kirby, J.T., Shi, F., 2016. Modeling wave-structure interactions by an immersed boundary method in a σ-coordinate model. Ocean Eng. 125, 238-247.

[11] Matsumura, Y., Hasumi, H., 2008. A non-hydrostatic ocean model with a scalable multigrid Poisson solver. Ocean Model. 24, 15-28.

[12] OpenCFD, OpenFOAM: The Open Source CFD Toolbox. User Guide Version 1.4, OpenCFD Limited. Reading UK, Apr. 2007.

[13] Smagorinsky, J., 1963. General circulation experiments with primitive equations. Mon. Weather Rev. 91, 99-164.

[14] Vitousek, S., Fringer, O.B., 2014. A nonhydrostatic, isopycnal-coordinate ocean model for internal waves. Ocean Model. 83, 118-144.